Slovak University of Technology in Bratislava
Institute of Information Engineering, Automation, and Mathematics

PROCEEDINGS

of the 18th International Conference on Process Control

Hotel Titris, Tatranská Lomnica, Slovakia, June 14 – 17, 2011

ISBN 978-80-227-3517-9

http://www.kirp.chtf.stuba.sk/pc11

Editors: M. Fikar and M. Kvasnica

Bobanac, V., Brekalo, M., Vašak, M., Perić, N.: Laboratory for Renewable Energy Sources and Identification of the Laboratory Wind Turbine Model, Editors: Fikar, M., Kvasnica, M., In *Proceedings of the 18th International Conference on Process Control*, Tatranská Lomnica, Slovakia, 470–478, 2011.

Full paper online: http://www.kirp.chtf.stuba.sk/pc11/data/abstracts/079.html

Laboratory for Renewable Energy Sources and Identification of the Laboratory Wind Turbine Model

V. Bobanac* M. Brekalo M. Vašak*** N. Perić******

Faculty of Electrical Engineering and Computing, University of Zagreb, Unska 3, HR-10000 Zagreb, Croatia
** (Tel: +385-1-6129805; e-mail: vedran.bobanac@fer.hr)*
*** (Tel: +385-34-263248; e-mail: brekalomarijan@gmail.com)*
**** (Tel: +385-1-6129821; e-mail: mario.vasak@fer.hr)*
***** (Tel: +385-1-6129863; e-mail:nedjeljko.peric@fer.hr)*

Abstract: This paper presents Laboratory for Renewable Energy Sources (LARES) at the Faculty of Electrical Engineering and Computing, University of Zagreb, Croatia. Laboratory consists of experimental setups for wind energy, solar energy and hydrogen fuel. The aim of LARES is development and experimental research of the advanced control strategies, in order to improve the energy conversion efficiency and thus increase the cost effectiveness of renewable energy sources. Focus of this paper is placed on the wind part of LARES and especially on mathematical model identification of the laboratory wind turbine. Obtained model is a basis for subsequent development of the wind turbine control algorithms.

1. INTRODUCTION

One of the main concerns of today's civilization is electrical energy production. The society, the more developed it is, consumes more energy. Therefore, growth of human population and development of societies imply increased energy demand. This trend will surely be continued in the future. Current world energy production is still based on burning of fossil fuels which becomes more and more unacceptable, mainly because of the current levels of related CO_2 emissions which cause ecological problems. On the other hand fossil fuel reserves will sooner or later be exhausted. In last two decades numerous international agreements and protocols have been signed, which oblige the signing countries to reduce the CO_2 emissions. Thus, many governments are forced to subsidize development and building of the ecologically acceptable power plants. These are all reasons why investment in renewable energy sources have been growing rapidly in the last decade. EU members have set a goal that by the year of 2020 20% of total electrical energy production should come from renewable energy sources. According to the latest information from European Wind Energy Association (http://www.ewea.org/ 2011), this goal will be exceeded. Renewable energy source with the highest growth rate and potential for further development is the wind energy.

However, renewable energy is still not rentable like energy obtained from classical sources (e.g. thermal power plants). With the development of many new power plants based on renewable energy sources, one might rightfully raise a question about the energy conversion efficiency. The aim of the Laboratory for Renewable Energy Sources (LARES) on Faculty of Electrical Engineering, University of Zagreb (UNIZG-FER) is development and experimental research of the advanced control strategies, in order to improve the energy conversion efficiency and thus increase the cost effectiveness of the renewable energy sources.

The paper is organized as follows. Section 2 describes LARES in whole and in Section 3 wind part of LARES is described in more detail. In Section 4 insight into the LARES wind turbine control system is given. Section 5 describes the wind turbine identification experiment and the identification results are given in Section 6. Conclusions are given in Section 7.

2. DESCRIPTION OF THE LABORATORY

LARES is placed on the top floor of the UNIZG-FER skyscraper and it consists of the following experimental units:

- Wind turbine setup placed in the air chamber and driven by a fan;
- An array of solar panels placed on the roof of the skyscraper (under construction);
- Hydrogen fuel cells stack with metal hydride storage supplied by an electrolyser.

Principle scheme of LARES is shown in Figure 1. From the scheme it is visible that the three main parts of LARES are actually connected in a microgrid. This microgrid conceptually operates as follows. Energy obtained from wind and sun is either transferred to the grid or it is used in an electrolyser in order to produce hydrogen which is then deposited in a metal hydride storage. In cases when energy from wind and sun is not sufficient, energy stored in hydrogen can be converted into electrical energy by using the fuel cells stack. The electrical energy is fed into the grid through properly controlled power converters.

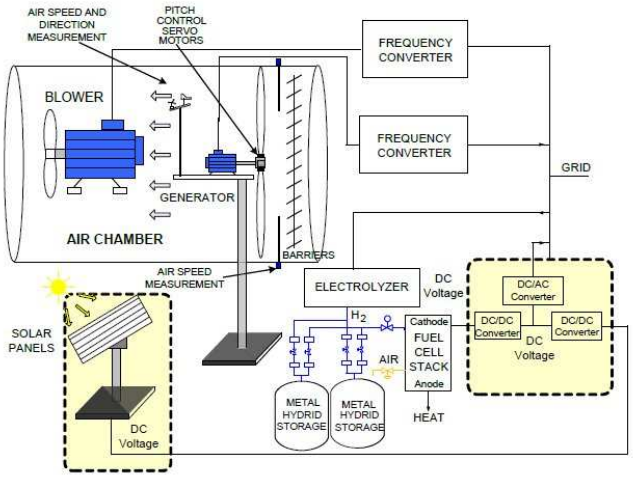

Fig. 1. Principle scheme of LARES.

The LARES configuration enables development and experimental research of control algorithms for each particular setup (wind, sun or hydrogen). The laboratory as a whole enables experimental research related to control of microgrids.

Layout of LARES is shown in Figure 2, where solar panels are not shown, as they are placed on the top of the skyscraper (just above the laboratory which is on the top floor).

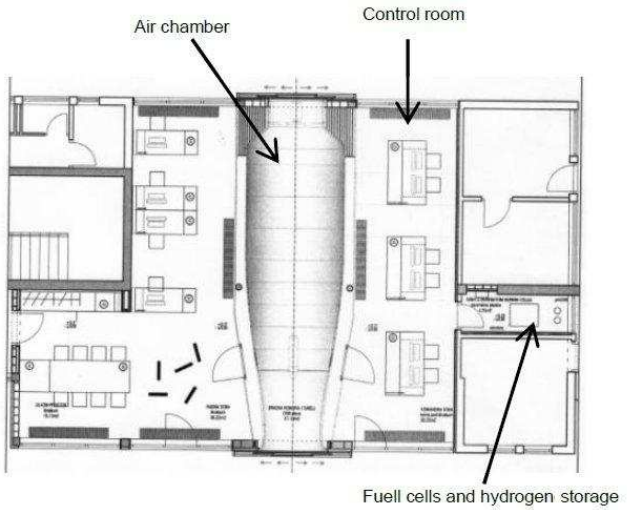

Fig. 2. LARES layout.

Focus of this paper is placed on the wind part of the laboratory, such that the rest of it relates only to the wind energy. In the following section a more detailed description of the wind turbine setup and of the air chamber is given.

3. WIND TURBINE AND WIND CHAMBER

Development and construction of the wind turbine setup was the most challenging task during the construction of the laboratory. The most important goal was the preservation of the aerodynamic relations present at MW-class wind turbines. The wind turbine setup design was initiated by extensive analysis and simulations in professional tools, where the basic requirements were (Perić et al. 2010):

- Preservation of Betz assumption regarding energy transformation;
- Fulfilling of dynamic, kinematic and geometry conditions;
- Respecting of optimal tip-speed ratio for three bladed rotor.

Laboratory wind turbine has rated power of 300 W and rated rotational speed of 240 rpm. Wind turbine setup is placed inside the wind chamber as shown in Figure 3.

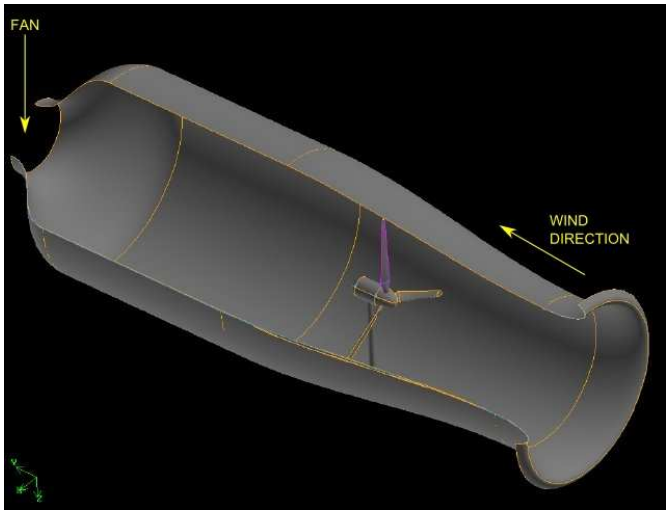

Fig. 3. Wind chamber layout.

The fan is placed at the far end of the chamber such that, when the wind is produced, the particles of air first pass across the turbine and then across the fan. Fan is controlled over the frequency converter which allows various rotational speeds of the fan and thus various wind speeds inside the chamber. This enables research of the wind turbine operation in wind conditions which are close to natural, where wind is stochastic.

Majority of the modern MW-class wind turbines are controlled by varying the generator torque and by pitching the rotor blades. This control structure was implemented on the laboratory wind turbine also. Since no commercially available small wind turbine could be used, completely new design had to be developed. This design included:

- 4-quadrant (4Q) frequency converter which is used for connecting the turbine synchronous generator to the grid;
- Actuators for pitching the rotor blades around their longitudinal axis.

4Q frequency converter allows electromagnetic torque of the turbine generator to be varied in a wide range which is used for control of the turbine rotational speed. Each of the three rotor blades has a DC servo drive which is used for pitching the blade around its longitudinal axis also for rotor speed control purposes. It is worth mentioning that laboratory turbine hub has a very limited space, so significant effort was needed to fit all of the components (servo motors, gearboxes, pitch controllers and blade position sensors). The issue of

control objectives and realization of the laboratory turbine control system is addressed in Section 4.

MW-class wind turbines due to their large dimensions have a flexible tower with low modal frequencies. In order to obtain plausible laboratory turbine model, flexible tower had to be constructed, which was not an easy task, since this demand comprises structural stability of the laboratory turbine. Solution was found in the form of the stiff tower which is mounted on an oscillatory bed and connected with the rigid structure through the system of springs and dampers. There are various types of springs and dampers and they can be replaced in order to obtain different tower characteristics.

Wind turbine and the wind chamber are also equipped with numerous sensors and instruments like: an array of 15 anemometers, torque sensor, accelerometers, strain gauges, web camera, stroboscope and weather station.

Realization of the wind turbine, the fan and the wind chamber is shown in Figure 4.

Fig. 4. Wind turbine setup in LARES.

Since aerodynamic relations present on the MW-class wind turbines were successfully transferred to the laboratory wind turbine and since all the means for controlling MW-class turbines were implemented on the laboratory turbine, it can be concluded that the design was successful and that the wind turbine setup can serve its primary purpose: development and research of the advanced control algorithms which can subsequently be implemented on the real, MW-class wind turbines.

4. WIND TURBINE CONTROL SYSTEM

Nonlinear relation between power in the wind and the wind speed (Jelavić et al. 2009) has resulted in modern wind turbines having two main operating regions: below rated wind speed and above rated wind speed. Rated wind speed is defined as the lowest wind speed at which wind turbine is operating at its rated power.

Below rated wind speed power that can be extracted from the wind is smaller than the rated power of the wind turbine and the control objective in this region is to maximize energy conversion efficiency. Control is performed by adjusting the generator torque, while the pitch angle is kept around minimum value of 0^o, such that the system operates along the maximum power coefficient curve (Jelavić et al. 2009). Controlling the generator torque is possible because modern generators are not connected to the grid directly, but over a frequency converter which allows generator speed to be varied in a wide range. Wind turbines with synchronous generator that is connected to the frequency converter of rated generator power are particularly suitable for such control strategy. The wind turbine setup in LARES is constructed such that it satisfies these characteristics.

Above rated wind speed power that can be extracted from the wind grows rapidly with the wind speed and it is greater than the rated power of the wind turbine. Control objective in this region is to limit the turbine rotational speed on its rated value which implies that the wind turbine is operating at the rated power. This is the case because generator torque is kept at the rated value above rated wind speed. Control in this region is performed by pitching the rotor blades which changes aerodynamic characteristics of the blades in order to lower the energy conversion efficiency. This degradation is necessary as the wind turbine generator should not operate above its rated power.

Explanation given above describes basic principles of classical control system for modern wind turbines, structure of which is shown in Figure 5.

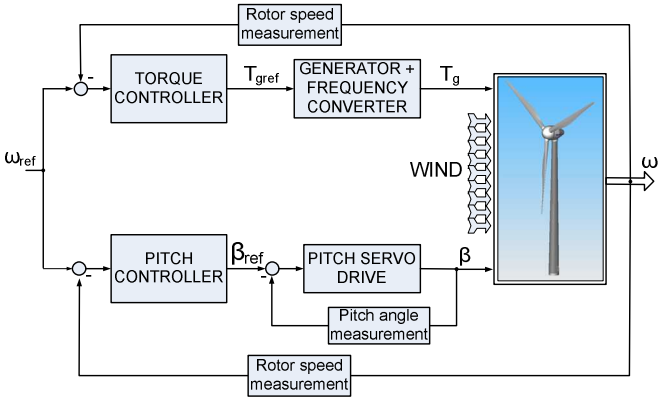

Fig. 5. Classical wind turbine control system.

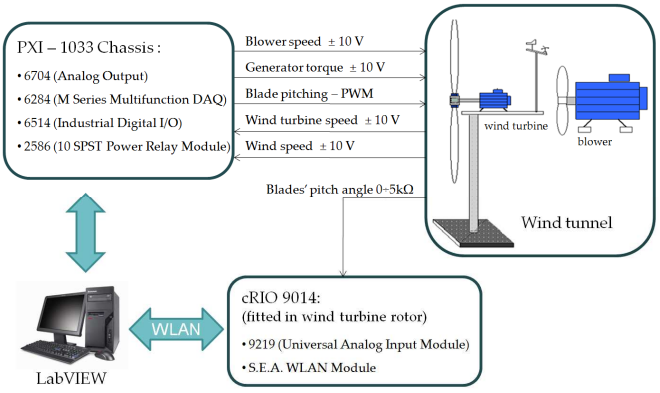

Fig. 6. Principle scheme of the wind turbine control system in LARES.

The laboratory wind turbine control system is based on platform LabVIEW (Laboratory Virtual Instrumentation Engineering Workbench) (National Instruments 2007), and it is implemented on a PC. All signal processing and control computational tasks are performed on a PC, while data acquisition and signal generation are performed on specialized input-output circuitry, produced also by National Instruments. Principle scheme of the laboratory wind turbine control system is shown in Figure 6.

The equipment for signal generation and acquisition can be divided into two groups:

- PXI-1033 chassis which is used for communication between the PC and the input-output modules;
- cRIO-9014 controller used for blade pitch angle measurement.

PXI-1033 chassis contains 4 modules over which various analog and digital signals are measured and generated. Some of the most important signals are: analog output signals for defining the fan speed and generator electromagnetic torque, analog input signals of measured generator speed and rotor position, output PWM signals for pitching of each of the turbine blades, digital output signals for starting the fan and the generator, digital input signals which indicate state of the plant (fan works, generator ready…) etc.

cRIO-9014 is mounted in the turbine rotor together with 3 potentiometer sensors for measuring blade pitch angles. cRIO consists of modules which are programmed to periodically collect the measured data and send it to PC by a WLAN protocol.

Configuration of the laboratory wind turbine control system allows both classical and advanced control strategies to be implemented and tested. Wind turbine and wind farm control has been one of the main research interests at UNIZG-FER for past ten years. In this period many advanced wind turbine control and estimation algorithms have been developed or upgraded. For instance, one such algorithm is individual blade pitch control which can significantly reduce the mechanical loads on the turbine construction (Jelavić et al. 2008). So far these algorithms have been tested using professional simulation tools such as GH Bladed (Jelavić et al. 2008, 2009). Now these algorithms can be tested on a laboratory turbine where all the problems present in real systems can be considered. This is one step closer to the final goal which is implementation of the advanced control algorithms on real MW-class wind turbines.

5. IDENTIFICATION PROCEDURE

Basis for designing a control system is a reliable mathematical model of a process that is to be controlled. One way of obtaining a mathematical model is theoretical analysis and setting the equations which describe behavior of the process (e.g. equations of energy and momentum balance). Such a model of a laboratory wind turbine has already been obtained (Jelavić et al. 2009) and it has been used for design of various control algorithms and for testing of these algorithms in simulations. However, when it comes to real, practical systems a more reliable mathematical model may be obtained by process identification. Process identification is another way of obtaining a mathematical model, which is based on processing and analysis of input/output data obtained on the real process. Identification of the laboratory wind turbine mathematical model is described in the sequel.

It has been decided to use a parametric method of identification and to search for a mathematical model in a state-space form, since this form is appropriate for subsequent advanced control system design. Also, the state-space model form is a good choice for identification of processes with unknown structure, because it requires only two parameters: model order and input delays (MathWorks 2010). Since the process is nonlinear (Jelavić et al. 2009) it cannot be described with a single linear mathematical model. Therefore, identification is performed in 4 operating points which are defined by the wind speed. For each operating point a linear mathematical model in state-space form is obtained. Inputs to the system are wind speed (kept constant for a certain operating point), generator torque and pitch angle, while the output is turbine rotational speed, as shown in Figure 5.

Identification is performed in 2 operating points below rated wind speed and in 2 operating points above rated wind speed. Transfer function (1) is obtained below rated and transfer function (2) above rated. This is reasonable since in classical control configuration generator torque and pitch angle are solely used for control in operating regions below and above rated wind speed, respectively (see Section 4).

$$G_T(z) = \frac{\omega(z)}{T_{gref}(z)} \tag{1}$$

$$G_\beta(z) = \frac{\omega(z)}{\beta_{ref}(z)} \tag{2}$$

Identification procedure includes the following steps:

1. Gathering of a-priori knowledge and information about the process;
2. Selection of the input test signal;
3. Imposing the test signal to the system and measurement of the input/output signals;
4. Obtaining mathematical model by processing of the recorded input/output data with the identification software;
5. Validation of the obtained mathematical model.

In the sequel these steps are described in more detail.

Step 1.

A-priori knowledge about the wind turbine process is gathered from a theoretically obtained nonlinear mathematical model. This model was previously obtained for the MW-class wind turbine (Jelavić et al. 2009) and it was subsequently adjusted to suit the laboratory turbine. The model is implemented both in Matlab and LabVIEW. By simulations of this model important information are obtained which are primarily used for selecting the test signal parameters. This is described in the following step.

Step 2.

Parametric identification is based on processing of the measured input/output data of the observed system. Therefore, selection of the proper input test signal is very important. In theory white noise is a very good test signal because it excites all the frequency modes of the system. This is important, because the resulting model should contain all of the system's important dynamics. Since white noise cannot be physically realized, for linear model identification PRBS (*Pseudo Random Binary Sequence*) is used instead. PRBS is a signal which has similar characteristics to the white noise. It is a rectangular signal of various width. It can take on only two values (*binary*) which change pseudo-randomly (*pseudo random*) at multiples of the sampling time. The pseudo random signal sequence repeats several times. PRBS signal was realized in LabVIEW by using shift register and an "exclusive OR" function.

Selection of PRBS parameters is vital for identification. Parameters that are to be selected are: c – amplitude, Δt – clock time (minimum length between signal changes) and N – number of clock times in a single period. Example of a PRBS signal is shown in Figure 7.

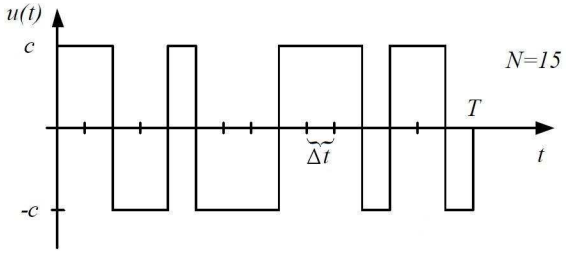

Fig. 7. Example of a PRBS signal – single period.

Following guidelines for determining parameters of a PRBS signal were taken from (Perić et al. 2005). Amplitude c is chosen depending on the process characteristics. It must be neither too small (because signal/noise ratio would then be too small) nor too large (because system can drift away from its operating point or nonlinear effects may be pronounced in responses). Clock time is chosen as approximately 1/5 of the smallest dominant system time-constant. N is chosen so that PRBS period T defined in (3) has a value about 50% larger than the system's impulse response settling time (t_{95}). Approximate relation is given in (4).

$$T = N \cdot \Delta t \tag{3}$$

$$T \approx 1.5 \cdot t_{95} \tag{4}$$

Number of repetitions of a PRBS signal is bounded by the allowed measurement time which is given by relation:

$$T_M = M \cdot T\,, \tag{5}$$

where M is the number of PRBS signal periods used in identification. Larger M is required for better signal/noise ratio.

Another important parameter for identification is sample time T_S. Sample time can be determined from the following empiric relation:

$$T_S = \left(\frac{1}{6} \div \frac{1}{10}\right) \cdot t_{63}\,, \tag{6}$$

where t_{63} relates to the system's step response rise time. When determining sample time one should bear in mind that Nyquist-Shannon sampling theorem must be satisfied for higher resonant frequencies. This can be controlled by determining frequency characteristics of the system, as described in (Brestovec 2005). It should be pointed out that the just mentioned frequency characteristics, as well as the impulse and step responses (for information about t_{95} and t_{63}) are determined from a theoretical mathematical model (this is the required a-priori knowledge about the system, which was mentioned in *Step 1*).

Step 3.

System must be brought to the desired operating point in closed-loop control. Once the system reaches the steady-state controllers are turned off and the test PRBS signal is imposed to the system input (torque or pitch reference depending on the operating point). During the experiment system output (turbine rotational speed) is recorded. Note that the identification is performed with control loop open (controllers are turned off during the identification data collection).

Step 4.

After the experiment is finished sets of the recorded input/output data are forwarded to the identification software. In this case Matlab's SIT (*System Identification Toolbox*) was used. SIT was configured to use parametric identification procedure shown in Figure 8.

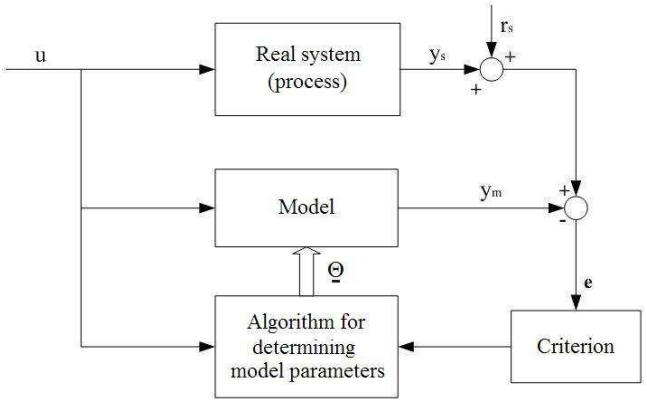

Fig. 8. Principle scheme of parametric identification procedure.

In the parametric identification procedure optimization methods are used to vary the set of model parameters, in order to minimize the difference between the model output and the measured output. Model order (and thus the number of model parameters) can be defined by the user.

Step 5.

After the model has been obtained it is validated on the set of data which is different from the one used for identification. Usually a step response is used for validation of the identified models. However, since our laboratory wind turbine setup is extremely sensitive to disturbances in the form of outer wind, it was impossible to obtain reliable, repeatable step responses on a real system. Therefore, data obtained during identification experiment was simply split in half, so that one half was used for identification (*Step 4*) and the other half for validation.

6. RESULTS

Before conducting the experiment on a real system, identification was carried out on a theoretically obtained mathematical model implemented on a LabVIEW platform. This was very useful to get acquainted with the steps of the identification procedure and the obtained results were very good (not shown in this paper).

After successful identification of the LabVIEW model, experiments on the real system could begin. It is worth mentioning that although transfer function from wind speed to turbine rotational speed, given by (7), would be very useful for predictive control system design, it could not be identified because of the fan protection system. Namely, a ramp filter has been put on the fan speed reference, so that the fan motor is protected from sudden speed changes. Therefore, it is not possible to produce the wind speed in the form of a PRBS signal.

$$G_v(z) = \frac{\omega(z)}{v_{wind}(z)} \tag{7}$$

During the experiment significant effort was needed to bring the system to the desired operating point and especially to achieve that the system does not drift away from the operating point once the controllers are turned off and the PRBS signal is imposed on the system inputs. The reason for this lies in nonlinearity of the system and also in a fact that the system is very sensitive to outer wind speed (wind that normally blows in the surroundings) and on rare occasions was the weather completely steady. Solution has been found in experimenting with PRBS parameters until the system was able to stay around the desired operating point long enough to record enough data, i.e. to achieve at least M=5 in relation (5). Although PRBS parameters were found by trial-and-error method, their initial value was determined from the recommendations given in Section 5 (*Step 2*). Specific parameters of the used PRBS signals will be given in the sequel for each particular operating point.

Sample time has also been determined along the guidelines from Section 5. It is fixed, i.e. it does not change with the operating point and it amounts 20 ms. It is also worth noting that all the identification experiments were conducted with stiff laboratory turbine tower, because the system of springs and dampers, which allows tower oscillations, was not yet fully functional at the time of experiments.

All identified linear state-space models are given in the following discrete-time form:

$$\begin{aligned} x(k+1) &= A \cdot x(k) + B \cdot u(k) + K \cdot e(k), \\ y(k) &= C \cdot x(k) + D \cdot u(k) + e(k). \end{aligned} \tag{8}$$

Here *x(k)* is a state vector. Dimension of *x(k)* corresponds to the model order. *u(k)* and *y(k)* are system input and output respectively. *K* is a matrix which models influence of the noise to the system and *e(k)* is process noise (white noise which is generated and used by the identification software). *A*, *B*, *C* and *D* are standard matrices used in the state-space form.

Free parameterization of the state-space matrices was used, which means that any elements in the matrices are adjustable by identification algorithm. Therefore, a basis for the state-space realization is automatically selected to give well-conditioned calculations (MathWorks 2010).

Based on the obtained input-output data, models were also identified in parametric forms other than state-space, e.g. ARX, ARMAX, BJ and OE. Identified models of different forms were mutually compared by validation and they all gave similar results (not shown in this paper).

Identification results for each of the 4 operating points are presented in the sequel. Since state-space models were identified results are presented in the form of state-space matrices, but also in the form of corresponding transfer functions. Models presented in Subsections 6.1 and 6.2 correspond to the transfer function (1), while models in 6.3 and 6.4 correspond to (2) (see Figure 5). For every operating point two figures are given. First one displays recorded input-output data, while the second one displays validation results. In all the figures mean values of the signals have been removed, but they are given in tables along with PRBS parameters used. Models of different orders were obtained and the ones that gave the lowest deviation from the real system are displayed. It is worth noting that responses of three identified models in Figure 10 overlap. By plotting pole/zero maps (not shown), it has been found that all the identified models are stable. It can be concluded that satisfactory results have been obtained, despite all the problems that are always present on real systems, e.g. nonlinearities, measurement noise, sensitivity to disturbances etc.

Additionally, pitch servo drive identification has been performed and the results are given in Subsection 6.5. In Figure 18 responses of the real pitch servo drive and the identified model are compared. The model describes the real system satisfactory and matching of the responses is good.

It should be pointed out that the identified models from Subsections 6.3 and 6.4 include the dynamics of the pitch servo drive. Since model (15) has order 3 and the pitch servo drive (17) has order 2, it can be argued how can the remaining part of the system (from β to ω, see Figure 5) be modeled with only first order. From (Jelavić et al. 2009) it can be seen that this is reasonable because the identification has been performed with the stiff tower.

6.1 Identification of $G_T(z)$ with v_{wind} = 7 m/s

Values of the process variables		PRBS parameters	
T_{mean} =	3.5 Nm	c =	0.8 Nm
β_{mean} =	0^o (const)	N =	16
ω_{mean} =	183 rpm	Δt =	1 s

Table 1. Identification parameters for v_{wind} = 7 m/s.

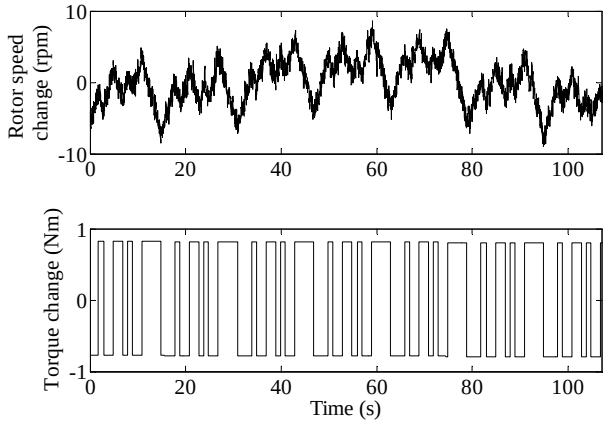

Fig. 9. Output and input signals for v_{wind} = 7 m/s.

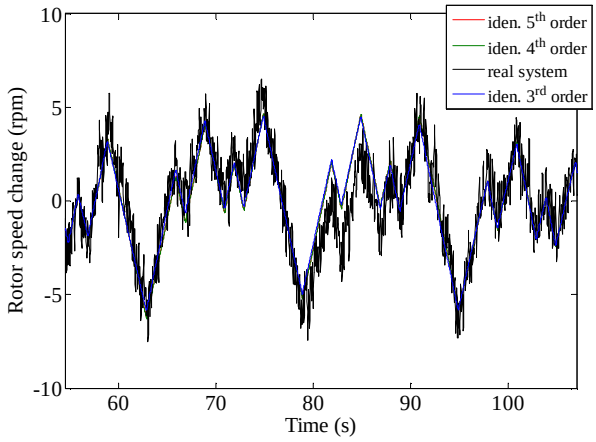

Fig. 10. Turbine rotational speed responses for v_{wind} = 7 m/s.

Identified 3rd order state-space model of structure (8) reads:

$$A=\begin{bmatrix} 0.99559 & 0.046808 & -0.065886 \\ -0.054331 & 0.63367 & -0.64621 \\ 0.012755 & 0.72281 & 0.7296 \end{bmatrix},$$
$$B=\begin{bmatrix} -0.00021549 \\ 0.0018215 \\ -0.0017577 \end{bmatrix},\quad K=\begin{bmatrix} 0.003357 \\ 0.016101 \\ -0.00023999 \end{bmatrix}, \qquad (9)$$
$$C=\begin{bmatrix} 371.12 & 6.5785 & -11.542 \end{bmatrix},$$
$$D=\begin{bmatrix} 0 \end{bmatrix}.$$

Corresponding transfer function reads:

$$G_{T1}(z)=\frac{-0.0477z^{-1}+0.1223z^{-2}-0.1081z^{-3}}{1-2.359z^{-1}+2.29z^{-2}-0.9299z^{-3}}. \qquad (10)$$

6.2 Identification of $G_T(z)$ with v_{wind} = 9 m/s

Values of the process variables		PRBS parameters	
T_{mean} =	4.9 Nm	c =	0.8 Nm
β_{mean} =	0^o (const)	N =	16
ω_{mean} =	213 rpm	Δt =	1 s

Table 2. Identification parameters for v_{wind} = 9 m/s.

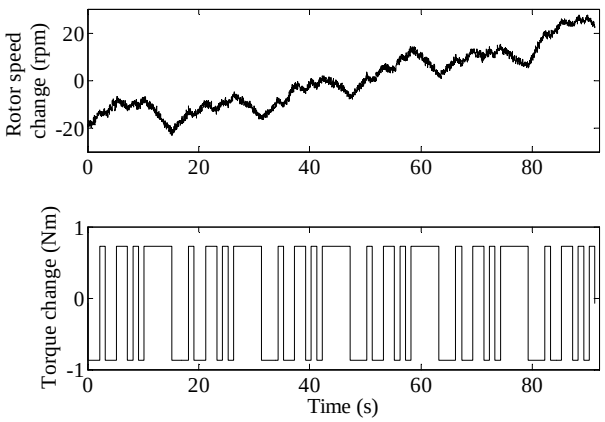

Fig. 11. Output and input signals for v_{wind} = 9 m/s.

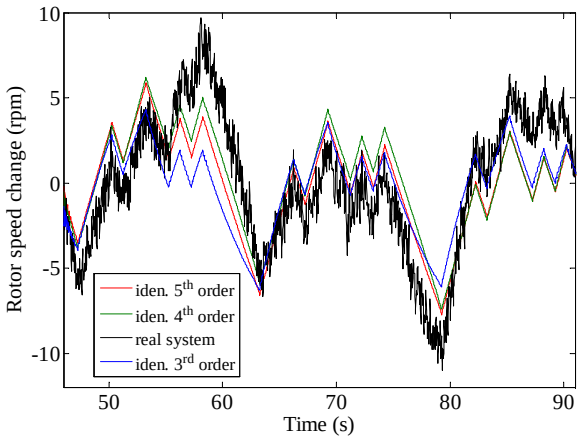

Fig. 12. Turbine rotational speed responses for v_{wind} = 9 m/s.

Identified 4th order state-space model of structure (8) reads:

$$A=\begin{bmatrix} 0.98208 & -0.16176 & -0.061514 & -0.068064 \\ 0.13113 & 0.51558 & 0.80396 & -0.29476 \\ -0.069255 & -0.73422 & 0.61965 & 0.25423 \\ -0.034816 & 0.13938 & 0.12753 & -0.19436 \end{bmatrix},$$
$$B=\begin{bmatrix} 0.00028043 \\ 0.00051794 \\ 0.0014344 \\ 0.002622 \end{bmatrix},\quad K=\begin{bmatrix} 0.0073324 \\ -0.016026 \\ 0.010136 \\ 0.019012 \end{bmatrix}, \qquad (11)$$
$$C=\begin{bmatrix} 181.66 & -12.455 & -5.863 & -2.6417 \end{bmatrix},$$
$$D=\begin{bmatrix} 0 \end{bmatrix}.$$

Corresponding transfer function reads:

$$G_{T2}(z)=\frac{0.02916z^{-1}-0.0843z^{-2}+0.04038z^{-3}-0.03675z^{-4}}{1-1.923z^{-1}+1.636z^{-2}-0.5914z^{-3}-0.1215z^{-4}}. \qquad (12)$$

6.3 Identification of $G_\beta(z)$ with v_{wind} = 11 m/s

Values of the process variables		PRBS parameters	
T_{mean} =	6.8 Nm (const)	c =	2^o
β_{mean} =	5.6^o	N =	32
ω_{mean} =	240 rpm	Δt =	2 s

Table 3. Identification parameters for v_{wind} = 11 m/s.

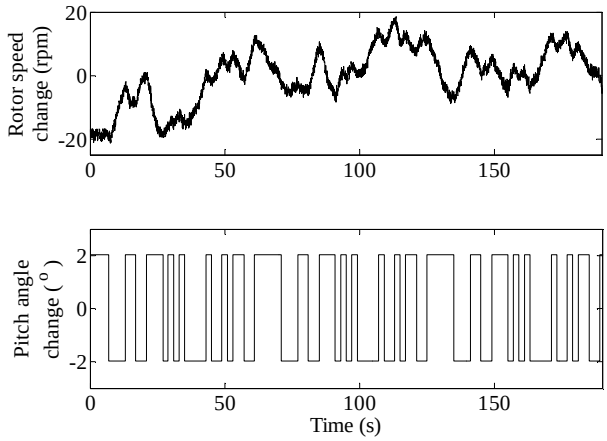

Fig. 13. Output and input signals for v_{wind} = 11 m/s.

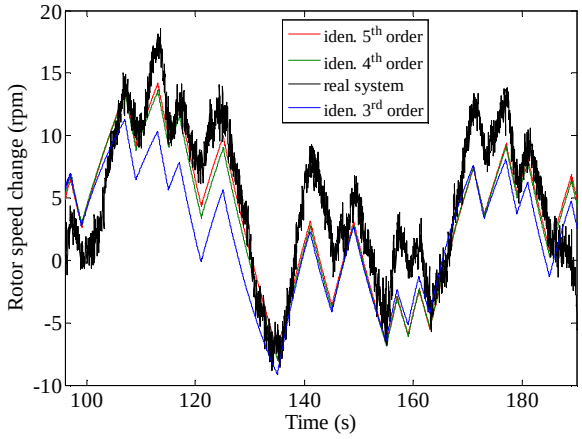

Fig. 14. Turbine rotational speed responses for v_{wind} = 11 m/s.

Identified 4th order state-space model of structure (8) reads:

$$A = \begin{bmatrix} 0.99592 & -0.068805 & 0.0048254 & 0.048758 \\ 0.045489 & 0.40068 & -0.90725 & -0.097681 \\ 0.026732 & 0.79103 & 0.30208 & 0.53587 \\ 0.036769 & 0.12396 & 0.36363 & -0.3416 \end{bmatrix},$$

$$B = \begin{bmatrix} 3.6982e-05 \\ -0.00014468 \\ 0.0013955 \\ -0.0024389 \end{bmatrix}, \quad K = \begin{bmatrix} 0.0018945 \\ -0.0060099 \\ -0.005948 \\ -0.010702 \end{bmatrix}, \quad (13)$$

$$C = [659.29 \quad -17.365 \quad 6.3086 \quad 12.757],$$

$$D = [0].$$

Corresponding transfer function reads:

$$G_{\beta 1}(z) = \frac{0.004584z^{-1} - 0.01992z^{-2} + 0.04688z^{-3} - 0.05696z^{-4}}{1 - 1.357z^{-1} + 0.7768z^{-2} + 0.03354z^{-3} - 0.4519z^{-4}}. \quad (14)$$

6.4 Identification of $G_\beta(z)$ with v_{wind} = 13 m/s

Values of the process variables		PRBS parameters	
T_{mean} =	6.8 Nm (const)	c =	2^o
β_{mean} =	10.7^o	N =	32
ω_{mean} =	240 rpm	Δt =	2 s

Table 4. Identification parameters for v_{wind} = 13 m/s.

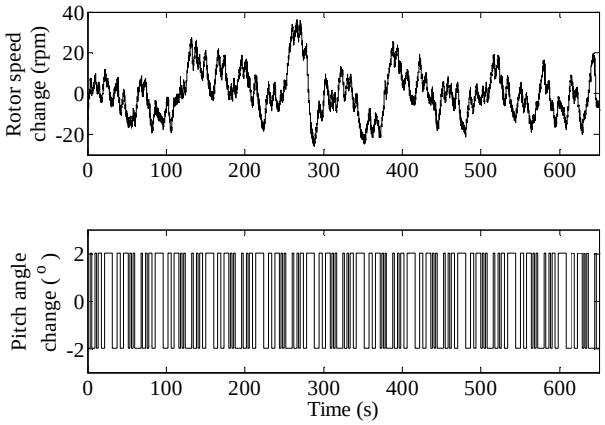

Fig. 15. Output and input signals for v_{wind} = 13 m/s.

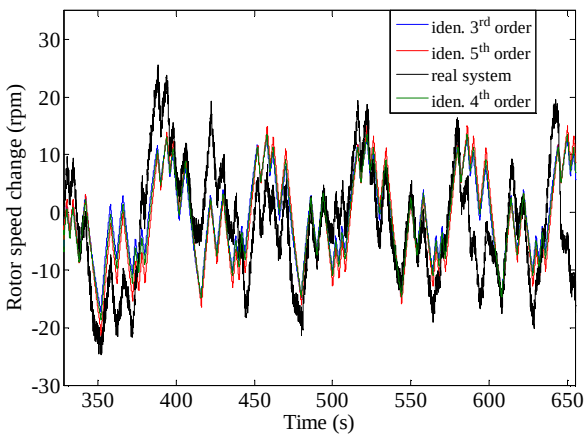

Fig. 16. Turbine rotational speed responses for v_{wind} = 13 m/s.

Identified 3rd order state-space model of structure (8) reads:

$$A = \begin{bmatrix} 0.99693 & -0.060215 & -0.026464 \\ 0.043779 & 0.45433 & 0.83324 \\ -0.0253 & -0.79544 & 0.55406 \end{bmatrix},$$

$$B = \begin{bmatrix} -9.1179e-006 \\ -0.00012523 \\ 6.5033e-005 \end{bmatrix}, \quad K = \begin{bmatrix} 0.00067204 \\ -0.0030013 \\ 0.0028048 \end{bmatrix}, \quad (15)$$

$$C = [1969.8 \quad -45.602 \quad -28.418],$$

$$D = [0].$$

Corresponding transfer function reads:

$$G_{\beta 2}(z) = \frac{-0.0141z^{-1} + 0.01811z^{-2} - 0.02716z^{-3}}{1 - 2.005z^{-1} + 1.922z^{-2} - 0.9151z^{-3}}. \quad (16)$$

6.5 Identification of the pitch servo drive

Task of the pitch servo drive is to position the rotor blades into the angular position required by the outer loop (see Figure 5). Dynamics of the pitch servo drive does not depend on the operating point (wind speed) and it turns out that it can be described by a second-order transfer function. Input-output data are shown in Figure 17. These data were recorded during identification experiment described in Subsection 6.4. Therefore all the parameters of the experiment are given in Table 4. above.

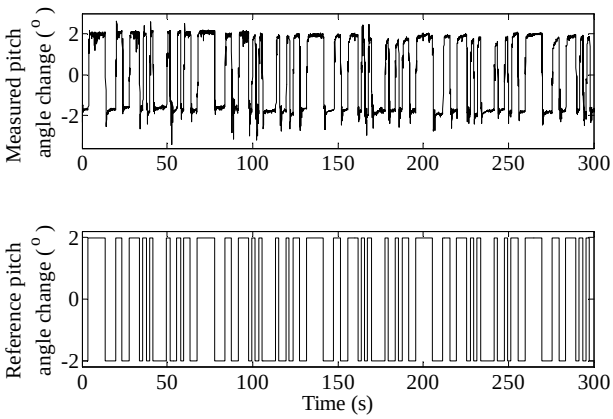

Fig. 17. Output and input signals of the pitch servo drive.

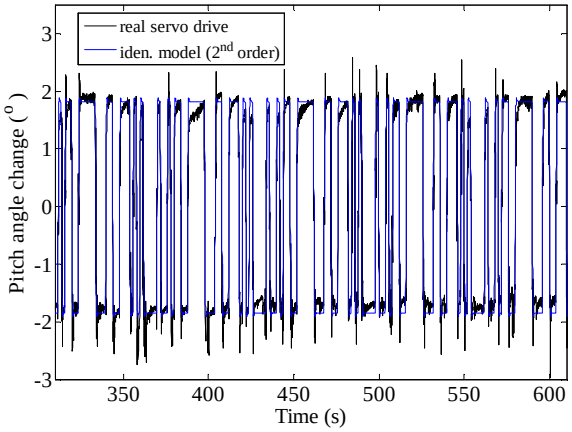

Fig. 18. Pitch servo drive responses.

Identified transfer function of the pitch servo drive is:

$$G_{servo}(z) = \frac{\beta(z)}{\beta_{ref}(z)} = \frac{0.006363z^{-1} + 0.004433z^{-2}}{1 - 1.876z^{-1} + 0.8881z^{-2}}. \quad (17)$$

7. CONCLUSION

Laboratory for Renewable Energy Sources on Faculty of Electrical Engineering and Computing, University of Zagreb enables experimental research and development of various advanced control algorithms for renewable energy sources. These algorithms can be used to enhance the electrical energy production from wind, sun and hydrogen, but also to reduce losses in a process of producing hydrogen which is used for storing energy.

Laboratory wind turbine setup, which has all the important characteristics of the modern MW-class wind turbines, is described. Identification of the laboratory wind turbine mathematical model has been performed and satisfactory results have been obtained. Reliable mathematical model of a process is a basis for successful control system design.

ACKNOWLEDGMENTS

This work has been financially supported by *The National Foundation for Science, Higher Education and Technological Development of the Republic of Croatia* and *Končar – Electrical Engineering Institute*.

REFERENCES

Bobanac V., M. Jelavić and N. Perić (2010). Linear Parameter Varying Approach to Wind Turbine Control, *Proceedings of the 14th International Power Electronics and Motion Control Conference EPE-PEMC 2010.*, 8 pages, Ohrid, Republic of Macedonia.

Brekalo M. (2010). *Mathematical Model Identification of the Laboratory Wind Turbine*, Master thesis, Faculty of Electrical Engineering and Computing, Zagreb, in Croatian.

Brestovec B. (2005). *Modeling Wind Turbines for the Purpose of Designing a Control System*, Master thesis, Faculty of Electrical Engineering and Computing, Zagreb, in Croatian.

Burton T., D. Sharpe, N. Jenkins and E. Bossanyi (2001). *Wind Energy Handbook*, John Wiley & sons, Chichester, UK.

European Wind Energy Association (2011). http://www.ewea.org/.

Jelavić M. and N. Perić (2009). Wind Turbine Control for Highly Turbulent Winds, *Automatika*, **Vol. 50**, No. 3-4, pp. 135-151.

Jelavić, M., V. Petrović and N. Perić (2008). Individual pitch control of wind turbine based on loads estimation, *Proceedings of the 34th Annual Conference of the IEEE Industrial Electronics Society (IECON 2008)*, pp. 228-234, Orlando, USA.

MathWorks (2010). *System identification Toolbox 7*, User's Guide.

National Instruments (2007). *Getting Started with LabVIEW*, User's Guide.

Perić N. and I. Petrović (2005). *Process identification*, Lecture notes, Faculty of Electrical Engineering and Computing, Zagreb, in Croatian.

Perić, N, Ž. Ban, M. Jelavić, B. Matijašević, S. Mikac, M. Kostelac and H. Domitrović (2010). *Wind turbine control research in Laboratory for renewable energy sources*, 7 pages, European Wind Energy Conference and Exhibition, EWEC, Warsaw, Poland.

Petrović, V, N. Hure and M. Baotić (2010). *Appliance of LabVIEW software for development of HIL wind turbine speed control structure*, 6 pages, MIPRO, Opatija, Croatia, in Croatian.

Skogestad S. and I. Postlethwaite (2005). *Multivariable Feedback Control*, John Wiley & Sons Ltd, Chichester, UK.